Human Alkyladenine DNA Glycosylase Uses Acid−Base Catalysis for Selective Excision of Damaged Purines†

Patrick J. O'Brien and Tom Ellenberger*

Department of Biological Chemistry and Molecular Pharmacology, Harvard Medical School, 240 Longwood Avenue, Boston, Massachusetts 02115

Received July 8, 2003; Revised Manuscript Received August 11, 2003

ABSTRACT: Human alkyladenine DNA glycosylase (AAG) protects against alkylative and oxidative DNA damage, flipping damaged nucleotides out of double-stranded DNA and catalyzing the hydrolytic cleavage of the *N*-glycosidic bond to release the damaged nucleobase. The crystal structure of AAG bound to a DNA substrate reveals features of the active site that could discriminate between oxidatively damaged or alkylated purines and normal purines. A water molecule bound in the active site adjacent to the anomeric carbon of the *N*-glycosidic bond is suggestive of direct attack by water, with Glu125 acting as a general base. However, biochemical evidence for this proposed mechanism has been lacking. The structure also fails to explain why smaller pyrimidine nucleosides are excluded as substrates from this relatively permissive active site that catalyzes the excision of a structurally diverse group of damaged purine bases. We have used pH dependencies, site-directed mutagenesis, and a variety of substrates to investigate the catalytic mechanism of AAG. Single-turnover excision of hypoxanthine and 1,N^6-ethenoadenine follows bell-shaped pH−rate profiles, indicating that AAG-catalyzed excision of these neutral lesions requires the action of both a general acid and a general base. In contrast, the pH−rate profile for the reaction of 7-methylguanine, a positively charged substrate, shows only a single ionization corresponding to a general base. These results suggest that AAG activates neutral lesions by protonation of the nucleobase leaving group. Glu125 must be deprotonated in the active form of the enzyme, consistent with a role as a general base that activates and positions a water nucleophile. Acid−base catalysis can account for much of the 10^8-fold rate enhancement that is achieved by AAG in the excision of hypoxanthine. The prominent role of nucleobase protonation in catalysis by AAG provides a rationale for its specialization toward damaged purines while effectively excluding pyrimidines.

DNA bases are subject to spontaneous alkylation and oxidative deamination events that change the structure and coding potential of DNA. The failure to repair these inevitable modifications can block DNA-templated activities such as replication and transcription or cause mutations during replication past damaged DNA. In human cells, a single enzyme, alkyladenine DNA glycosylase (AAG,[1] also known as methylpurine DNA glycosylase), is responsible for recognizing and initiating the repair of a variety of alkylated purines such as 3-methyladenine, 7-methylguanine (7MeG), and 1,N^6-ethenoadenine (ϵA) as well as hypoxanthine (Hx), a lesion caused by oxidative deamination of adenine (Scheme 1; for reviews, see refs *1* and *2*). AAG locates these relatively rare lesions among the vast excess of normal genomic DNA and initiates the base excision repair process by catalyzing the hydrolysis of the *N*-glycosidic bond to release the damaged base.

Crystal structures of AAG bound to a DNA substrate and an inhibitor have provided insights into the molecular features of DNA binding and the discrimination between normal purines and alkylated purines, and have identified candidate catalytic groups at the active site (*3*, *4*). From these structures, it is apparent that AAG utilizes nucleotide flipping to gain access to the *N*-glycosidic bond. The shape and electrostatic features of the pocket that accepts the flipped-out nucleotide suggest a basis for discrimination against unmodified purines. A steric clash between Asn169 and the exocyclic amino group of G could be responsible for discrimination against G, and an unfavorable interaction between the 6-amino group of A and the backbone amide of His136 could account for discrimination against A (*4*). However, the spacious binding pocket observed in the crystal structure should also be able to accommodate smaller pyrimidines, and yet pyrimidines are not substrates for this enzyme. Although AAG binds with

† This work was supported by an NRSA fellowship to P.J.O. (GM65043) and a grant to T.E. (R01 GM52504) from the National Institutes of Health. T.E. is the Hsien Wu and Daisy Yen Wu Professor of Biochemistry at Harvard Medical School.

* To whom correspondence should be addressed. E-mail: tome@hms.harvard.edu. Phone: (617) 432-0458.

[1] Abbreviations: 7MeG, 7-methylguanine; A, adenine; AAG, human alkyladenine DNA glycosylase; AlkA, *E. coli* 3-methyladenine DNA glycosylase; BSA, bovine serum albumin; C, cytosine; E, enzyme; ϵA, 1,N^6-ethenoadenine; G, guanine; Hx, hypoxanthine; k_{st}, rate constant for the single-turnover reaction with saturating AAG; NaCHES, sodium 2-(*N*-cyclohexylamino)ethanesulfonate; NaCAPS, sodium 3-(*N*-cyclohexylamino)-1-propanesulfonate; NaHEPES, sodium *N*-(2-hydroxyethyl)piperazine-*N*′-(2-ethanesulfonate); NaMES, sodium 2-(*N*-morpholino)ethanesulfonate; NaMOPS, sodium 3-(*N*-morpholino)propanesulfonate; PAGE, polyacrylamide gel electrophoresis; T, thymine; U, uracil.

10.1021/bi035177v CCC: $25.00
Published on Web 10/03/2003

Scheme 1

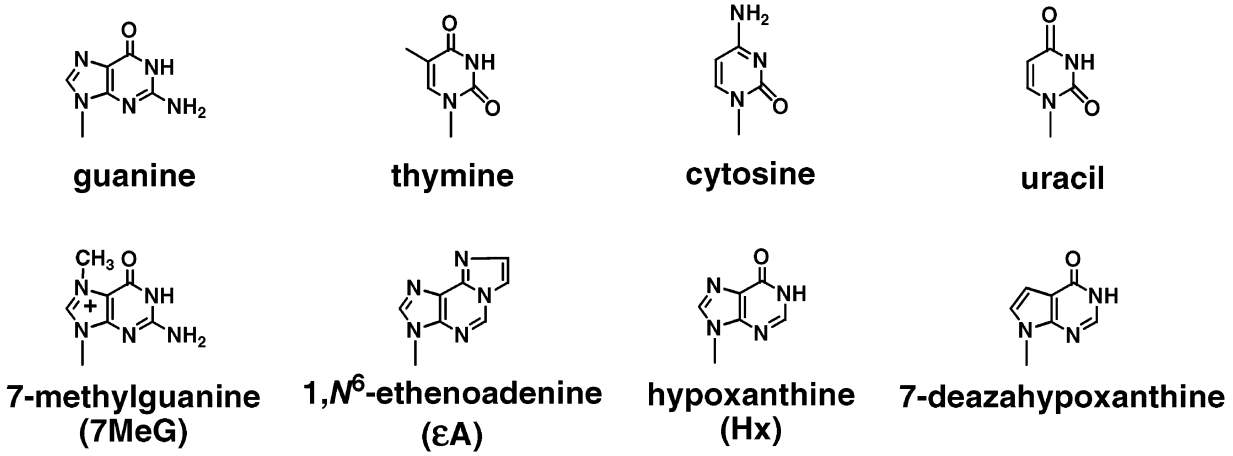

high affinity to pyrimidine·pyrimidine mismatches, it fails to catalyze their excision (*5*). This observation contrasts with the broader specificity of the *Escherichia coli* alkylation-specific DNA glycosylase AlkA that acts upon a variety of damaged purines and pyrimidines in DNA (*1*).

Although little is known about the catalytic mechanism of AAG or any other monofunctional DNA glycosylase that targets damaged purines, the corresponding nonenzymatic depurination reaction has been extensively characterized, and it provides a framework for investigating the enzymatic reaction mechanism (Figure 1). The observed kinetic isotope effects, pH dependencies, and structure−reactivity comparisons suggest that spontaneous depurination proceeds via *N*-glycosidic bond cleavage with an oxocarbenium ion-like transition state (*6*−*10*). This transition state is characterized by a large amount of bond cleavage to the purine leaving group, with an accumulation of positive charge on C1′ and O′ of the deoxyribosyl group, and only a small degree of bonding to the water nucleophile. A consequence of this dissociative transition state is that chemical activation of the nucleophile is expected to have only a modest stimulatory effect on the rate of reaction, whereas stabilization of the leaving group can provide a larger rate enhancement.

Correspondingly, the spontaneous hydrolysis of purine *N*-glycosidic bonds occurs by an efficient acid-catalyzed mechanism with protonation of the nucleobase at the N3 or N7 position (Figure 1). Indeed, the rate acceleration provided by protonation is so substantial that at neutral pH the reaction proceeds exclusively through the protonated form even though fewer than one in 10^5 molecules is protonated at this pH. Thus, much of the barrier to depurination can be explained by purines being poor leaving groups. This suggests that protonation would be a good catalytic strategy for enzymatic depurination at physiological pH. In contrast, pyrimidine bases are more difficult to protonate, and their hydrolysis is not acid-catalyzed in the pH range near neutrality. Correspondingly, the pyrimidine-specific uracil DNA glycosylase does not employ general acid catalysis (*11*, *12*). Although some similarities in the catalytic mechanisms of AAG and uracil DNA glycosylase might be expected on the basis of the similar oxocarbenium ion-like transition states observed for hydrolysis of purines and pyrimidines (*10*, *13*, *14*), AAG might be expected to take advantage of general acid catalysis in catalyzing the excision of purines.

We have used comparative pH−rate profiles, site-directed mutagenesis, and reactions with a variety of DNA substrates to obtain evidence for both acid and base catalysis in the AAG-catalyzed excision of damaged bases. The use of general acid catalysis can explain how AAG targets damaged purine nucleosides and excludes pyrimidine nucleosides. It would be difficult to sterically exclude the smaller pyrimidine bases from binding to the active site pocket of AAG, which is designed to accommodate a structurally diverse set of modified purines. However, the different shape and chemical properties of a bound pyrimidine would not be amenable to an acid-catalyzed mechanism that was designed for purine substrates. AAG appears to achieve efficient catalysis toward damaged purines via a combination of nucleophilic activation/positioning and leaving group protonation within an active site that is not tailor-made for a single substrate.

EXPERIMENTAL PROCEDURES

Expression and Purification of Recombinant AAG. The Δ79 catalytic fragment of AAG lacking the first 79 amino acids was expressed in *E. coli* BL21(DE3) (Novagen) and purified according to the previously published protocols (*3*, *4*). Full-length AAG was cloned into a modified pET19b (Novagen) expression vector encoding an N-terminal 10-His tag and a linker that contains the recognition site for rhinovirus 3C protease (provided by T. Biswas) and expressed in *E. coli* strain C41 (*15*). Typically, cells were grown at 37 °C until they reached an optical density of ∼0.5 at 600 nm. They were then cooled to ∼16 °C in an ice bath, transferred to a 16 °C shaker/incubator, and induced with 100 μM IPTG. Protein expression proceeded for 12−16 h, and then cells were harvested and frozen at −80 °C. The AAG protein was purified by metal affinity chromatography using a His tag that was subsequently cleaved with rhinovirus 3C protease to produce full-length AAG with an additional Gly-Pro-His sequence N-terminal to the initiator methionine of the native protein. Subsequent ion exchange chromatography (Source S, Pharmacia) and gel filtration (S100, Pharmacia) yielded a protein that was greater than 99% pure as judged by SDS−PAGE with Coomassie staining. A new construct was created for expression of site-directed mutants of AAG with an N-terminal His tag to facilitate purification. The His-tagged catalytic domain of AAG, Δ80, was generated by PCR and cloned into the pET19b vector, and the

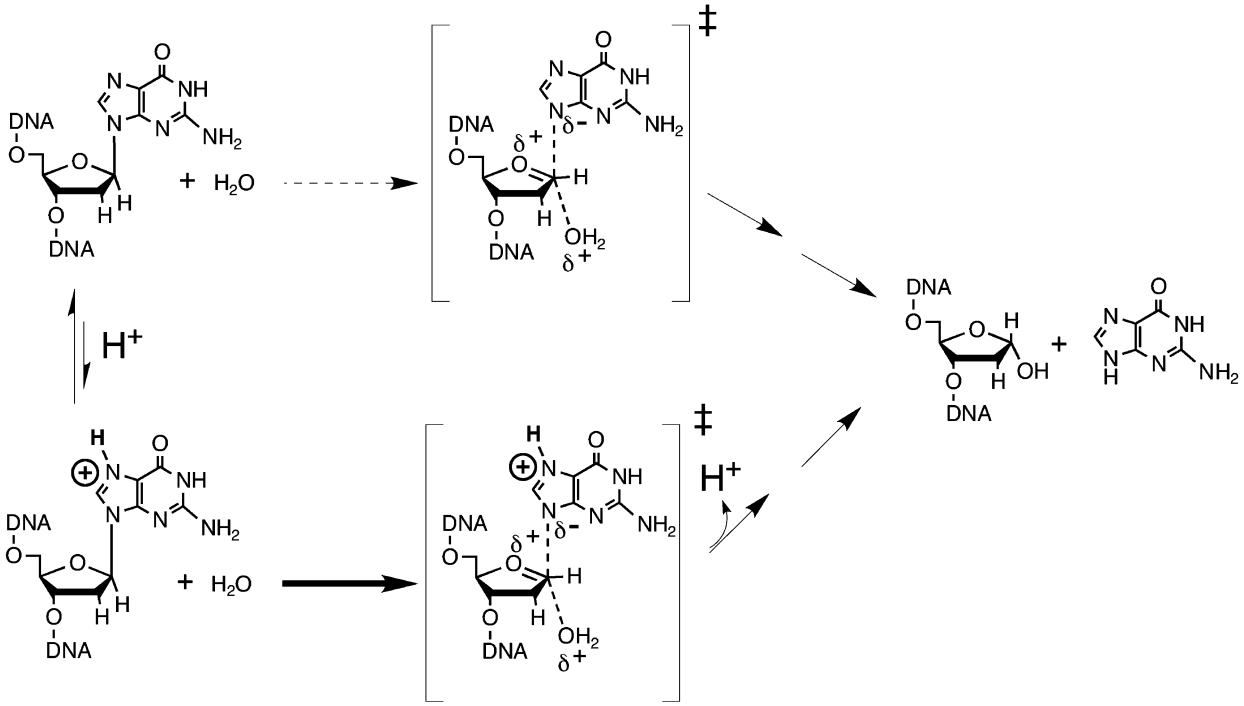

FIGURE 1: Spontaneous depurination is acid-catalyzed. Two possible pathways for the hydrolytic release of guanine from DNA are shown. Despite the unfavorable equilibrium for protonation at neutral pH, the acid-catalyzed reaction (bottom pathway) is overwhelmingly favored over the reaction of neutral guanosine (top pathway). A preponderance of physical organic data supports an oxocarbenium ion-like transition state for *N*-glycosidic bond cleavage in which the bond to the leaving group is largely broken and there is little formation of bonds to the incoming nucleophile. The acid-catalyzed pathway is preferred because protonated guanine (p$K_a \sim 7$) is a better leaving group than neutral guanine (p$K_a \sim 12$). After cleavage of the *N*-glycosidic bond, several rapid proton rearrangements are required to generate the deoxyribosyl (abasic) oligonucleotide and neutral (protonated) guanine products.

sequence was verified. This protein was expressed in *E. coli* BL21 RP codon plus (Stratagene) at 16 °C and purified via the same protocol used above for the His-tagged full-length protein. Proteolytic digestion with recombinant rhinovirus 3C protease left the nonnative N-terminal sequence $G^{80}P^{81}H^{82}M^{83}$ (the native sequence is $K^{80}G^{81}H^{82}L^{83}$). Site-directed mutants were constructed via the QuikChange method (Stratagene), and the coding region was verified by sequencing. The mutant AAG proteins were expressed and purified as described above for Δ80 AAG. The concentration of Δ80 AAG was determined from the calculated extinction coefficient ϵ_{280} of 2.5×10^4 M^{-1} cm^{-1}.

Preparation of Oligonucleotides. Oligonucleotides were synthesized on an ABI 394 DNA synthesizer using the standard 2-cyanoethyl (CE) phosphoramidite methodology according to manufacturers' recommendations. All reagents and phosphoramidites were obtained from Glen Research, except for the 7-deaza-2′-deoxyinosine CE-phosphoramidite (ChemGenes). After deprotection (24 h at 22 °C for ϵA-containing oligonucleotides or 8 h at 55 °C for unmodified oligonucleotides), oligonucleotides were purified by denaturing PAGE and the concentrations determined from the calculated extinction coefficient. The purity was evaluated by 5′-kinasing and denaturing PAGE. For activity or binding assays, the oligonucleotides were labeled on their 5′ ends with T4 polynucleotide kinase, purified by phenol/chloroform extraction, desalted with G-25 spin columns (Pharmacia), and subsequently annealed with a 2−3-fold molar excess of the complementary oligonucleotide. The 25mer oligonucleotide duplexes employed in this study corresponded to the following sequence, in which X is the position of the modified nucleotide substrate and Y is the opposing nucleotide.

X•Y	5'-CGA TAG CAT CCT **X**CC TTC TCT CCA T
	3'-GCT ATC GTA GGA **Y**GG AAG AGA GGT A

An enzymatic method was employed to create a 7MeG-containing oligonucleotide, as this compound is not available as a phosphoramidite (*16*). The primer 5′-CGATAGCATC-CT was annealed to the complementary 25mer oligonucleotide (Y is C, above) and extended with the Klenow fragment of DNA polymerase I in the presence of 7-methyldeoxyguanosine triphosphate (Sigma), dCTP, dTTP, and dATP as previously described (*16*). After extension, the reaction was quenched with 10 mM EDTA, the polymerase was removed with phenol/chloroform extraction, and the buffer was exchanged with a G-25 spin column. To obtain 7MeG mismatches, a 100-fold excess of the complementary strand (Y is T, A, or G) was added, and the oligonucleotide was denatured via brief thermal denaturation (3 min at 90 °C) and allowed to reanneal. A control annealing reaction, with a 100-fold excess of the DNA oligonucleotide complementary to the template (X is G), was used to generate a single-stranded oligonucleotide containing 7MeG. Native PAGE analysis confirmed that this procedure resulted in duplex DNA in the case of the mismatches, and single-stranded DNA in the case of the control reaction. The 20-fold greater rate of AAG-catalyzed excision of 7MeG•T than of 7MeG•C strongly suggests that the mismatched substrate was generated.

^{32}P-Based Glycosylase Assay. A ^{32}P-based alkaline cleavage and denaturing PAGE assay was used to quantify the

fraction of abasic product formed in glycosylase assays (*17*). Annealed oligonucleotide duplexes containing one 5′-^{32}P-labeled strand were incubated with AAG. At various times, a small aliquot was withdrawn and the reaction quenched with a larger volume of NaOH to obtain a final concentration of 0.2 M NaOH. Control reactions showed that the quench rapidly extinguished all glycosylase activity. Quenched samples were heated to 70 °C for 10 min to completely cleave the abasic product. After alkaline cleavage, samples were diluted with 1−2 volumes of gel loading buffer (98% formamide and 10 mM EDTA containing xylene cyanol FF and bromophenol blue dyes). The fraction of cleaved product at each time point was determined by separating the unreacted product and the shorter cleaved product in 15−20% denaturing polyacrylamide gels and quantifying the amount of radioactivity in each band using a Fuji BAS1000 phosphorimager.

Single-Turnover Assay for Glycosylase Activity. To ensure single-turnover reactions, the concentration of AAG was kept in excess of the concentration of labeled DNA (∼1 nM). For the determination of k_{cat}/K_m, the enzyme concentration was varied over a wide range to determine the K_m for the reaction. Although we refer to the $K_{1/2}$ for maximal activity as K_m, it should be noted that the $K_{1/2}$ for the single-turnover reaction is not necessarily the same as the K_m for the multiple-turnover reaction because the latter can be affected by the rate of product release. Once the K_m value for a given substrate and set of reaction conditions was determined, two or three concentrations of enzyme were chosen that were at least 10-fold below the K_m value. Under these conditions, the observed rate constant was linearly dependent upon the concentration of the enzyme. At least four independent determinations at two or more concentrations of enzyme were averaged to obtain the k_{cat}/K_m value ($k_{cat}/K_m = k_{obs}/[E]$ for conditions in which $[E] \ll K_m$). It should be noted that the reported k_{cat}/K_m values are for single-turnover conditions, but the measurement is analogous to the steady state k_{cat}/K_m. For the determination of k_{st}, the concentration of enzyme was varied over a range of 10−100-fold above the K_m to ensure saturation. The reported values of the single-turnover rate constant (k_{st}) are the average of at least three independent determinations. Preincubation controls in which AAG was incubated at 37 °C in the absence of substrate revealed that the enzyme is susceptible to inactivation within minutes to hours under the standard reaction conditions (50 mM buffer, 10% glycerol, 1 mM EDTA, and 1 mM DTT with an ionic strength adjusted to 100 mM with NaCl). This loss of activity could be overcome at high AAG concentrations (≥1 μM) by employing prelubricated microcentrifuge tubes as reaction vessels (Sorenson BioScience, Inc.), but the loss of activity persisted with more dilute solutions of AAG (≤50 nM). Incubations with a variety of different additives revealed that BSA (0.1 mg/mL), ovalbumin (0.1 mg/mL), or NP-40 (0.1%) could each stabilize even very low concentrations of AAG (∼1 nM) for more than 24 h at 37 °C, with no effect on the single-turnover kinetics of the glycosylase reaction (data not shown). Therefore, reactions employing low concentrations of AAG were supplemented with 0.1 mg/mL BSA.

pH Dependence. Reactions were typically carried out in 50 mM buffer, with 1 mM EDTA, 1 mM DTT, and 0.1 mg/mL BSA, at an ionic strength kept constant at 150 mM by the addition of NaCl. Preincubation controls (3−12 h) showed that the enzyme retained full activity under these conditions from pH 5 to 10. If a preincubation control showed a loss of activity, as was typical below pH 5, these data were not included in the pH dependence. The concentration of buffer was also varied while the ionic strength was kept constant, and different buffers were used at the same pH value to test for buffer-specific effects on AAG. No significant buffer effects on enzymatic activity were observed for the following buffers that were used at the indicated pH values: sodium acetate at pH 4.0−6.0, NaMES at pH 5.5−7.0, NaMOPS at pH 6.5−8.0, NaHEPES at pH 7.0−8.0, NaBicine at pH 8.0−9.3, NaCHES at pH 8.5−10.1, and NaCAPS at pH 9.0−10.0. At least three independent measurements were made at each pH value, and the average is reported. Unless otherwise indicated, the standard deviation of the mean was ≤15% of the value of the mean.

Scheme 2

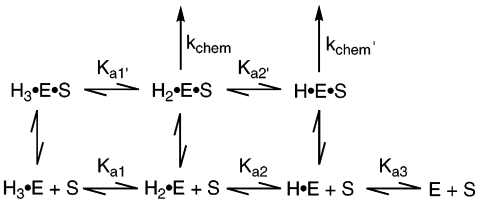

All of the pH−rate profiles were analyzed according to Scheme 2. Although three essential ionizations were observed for subsaturating DNA (i.e., k_{cat}/K_m conditions; pK_{a1}−pK_{a3}), only two essential ionizations were observed for saturating DNA (i.e., k_{st} conditions; p$K_{a1'}$ and p$K_{a2'}$). Two different chemical steps are shown, because for the single-turnover excision of 7MeG only a single ionization was observed, and therefore, this reaction could occur from the H_2•E•S complex (k_{chem}), from the H_3•E•S complex ($k_{chem'}$), or from both complexes with equal efficiency ($k_{chem} = k_{chem'}$). The H_2•E•S complex is the more reactive species for the single-turnover excision of Hx and ϵA.

The pH dependence of the reaction rate at a saturating enzyme concentration (k_{st}) was fit by eq 1 in the cases for which a single ionization was observed, and by eq 2 in the cases for which two ionizations were observed, using nonlinear regression analysis (Kaleidagraph). Similarly, the pH dependence of the second-order reaction at a subsaturating enzyme concentration (k_{cat}/K_m) was fit by eqs 3 and 4 for cases in which two or three ionizations were observed. As the E125C mutant retains some activity at low pH (∼70-fold less activity at pH 5 than at pH 9), this pH dependence was fit by eq 5, in which k_{st}^{min} reflects the rate constant for reaction of the protonated E125C (thiol) and k_{st}^{max} reflects the rate constant for reaction of the deprotonated E125C enzyme (thiolate).

$$k_{st} = k_{st}^{max}/(1 + [H^+]/K_{a'}) \quad (1)$$

$$k_{st} = k_{st}^{max}/(1 + [H^+]/K_{a1'} + K_{a2'}/[H^+]) \quad (2)$$

$$k_{cat}/K_m = (k_{cat}/K_m)^{max}/(1 + [H^+]/K_{a1} + K_{a2}/[H^+]) \quad (3)$$

$$k_{cat}/K_m = (k_{cat}/K_m)^{max}/(1 + [H^+]/K_{a1} + K_{a2}/[H^+] + K_{a2}K_{a3}/[H^+]^2) \quad (4)$$

$$k_{st} = k_{st}^{min} + k_{st}^{max}/(1 + [H^+]/K_{a1'}) \quad (5)$$

In all cases, an order of addition control was carried out in which either DNA substrate or enzyme was added first to the reaction mixture. Surprisingly, the E125D and E125C mutants reproducibly gave increased activity (5−7-fold) if the enzyme was diluted and incubated for 10 min at 37 °C prior to the addition of DNA. No such stimulation of glycosylase activity was observed for wild-type AAG. The values that are reported reflect the preincubated enzyme, but the apparent pK_a values were not significantly affected by the preincubation (data not shown). To facilitate measurement of the pH dependence for excision of Hx, these data were measured at 23 °C, whereas all other pH dependencies were determined at 37 °C.

AAG-Catalyzed Excision of Unmodified Pyrimidines and Purines. Binding of oligonucleotide duplexes containing central pyrimidine·pyrimidine mismatches was tested by electrophoretic mobility shift assays (C·C, T·C, T·T, U·T, and U·C), as previously described (*17*). These mismatches bound with similar affinity (K_d = 2−20 nM; data not shown). The pyrimidine·pyrimidine mismatch-containing duplexes were also assayed for glycosylase activity at pH 6 and 8, as described above. No hydrolysis products were detected after 2 days. As 1% product could have been easily detected, this places an upper limit on the rate constant for excision of pyrimidines of $\sim 3 \times 10^{-6}$ min^{-1} (0.01/48 h). Control experiments in which the enzyme was incubated in the absence of a substrate for 3 days prior to the addition of the substrate (ϵA·T) demonstrated that AAG retained full activity under these reaction conditions. In contrast, unmodified purines (G and A) are excised by AAG under identical reaction conditions when they were present as a mismatch. Although specific binding could not be detected by the gel shift assay for G·T or A·C duplexes, the AAG-catalyzed excision of G and A from these mismatches was saturable and exhibited K_m values similar to those for excision of Hx ($\sim$100 nM at an ionic strength of 100 mM).

Rate Enhancement for AAG-Catalyzed Excision of Hx. The rate enhancement is defined as the ratio of the enzymatic rate constant (k_{st}) divided by the nonenzymatic rate constant (k_{non}). The spontaneous rate of Hx release was measured at 55 and 70 °C, and the temperature dependence was extrapolated to 37 °C ($k_{non} = 1 \times 10^{-7}$ min^{-1}; data not shown). The single-turnover rate constant (k_{st}) for AAG-catalyzed excision of Hx at 37 °C and the same pH (6.0) equals 11 min^{-1} (data not shown). This gives a rate enhancement of 10^8 for the AAG-catalyzed hydrolysis of deoxyinosine [$k_{st}/k_{non} = 11$ min$^{-1}/(1 \times 10^{-7}$ min$^{-1}) = 10^8$].

RESULTS AND DISCUSSION

Characterization of the Δ80 Catalytic Fragment of AAG. These studies employed a carboxy-terminal fragment of AAG that contains the catalytic domain, because the full-length recombinant AAG protein is poorly soluble. This domain has a glycosylase activity identical to that of the full-length protein toward 3-methyladenine and hypoxanthine (*18*), and it has been crystallized in complex with DNA (*3*, *4*). The Δ80 AAG protein that we used in this study differs slightly from the previously characterized truncation mutant, Δ79 AAG (see Experimental Procedures), so we tested the catalytic activities of both proteins and compared them with the activity of full-length AAG. The single-turnover glycosylase reaction was used with a saturating enzyme concentration so that the observed rate constant reflects the single-turnover reaction of the substrate bound to the enzyme (k_{st}). This kinetic measurement is analogous to k_{cat} for a multiple-turnover reaction, but it does not include steps after the first irreversible step, such as product release, which can be rate-limiting for turnover of many DNA glycosylases (*19*, *20*). The Δ79, Δ80, and full-length AAG proteins have indistinguishable catalytic activities for single-turnover excision of either Hx or ϵA (see the Supporting Information). We refer to the Δ80 AAG enzyme hereafter simply as "AAG".

AAG Employs Acid−Base Catalysis. The pH dependence of an enzymatic reaction reveals the optimal conditions for assaying the enzyme, but more importantly, it provides insights about the protonation states of the substrate and of catalytic groups that are required for maximal activity. Knowledge of the active protonation state constrains possible catalytic mechanisms, and it can aid in the identification of catalytic groups. Nonenzymatic depurination of DNA occurs via acid-catalyzed protonation of the nucleobase, so it was of particular interest to determine if AAG utilizes a similar catalytic strategy. First, we compare the pH dependencies of the single-turnover reactions with different substrates to identify the essential ionization state of the E·S complex. We next examine the pH dependencies for k_{cat}/K_m, to probe the ionization of the free enzyme and substrate. Finally, we test candidate amino acids for their roles in the enzymatic reaction by characterizing the glycosylase activities of mutant proteins.

The pH dependence for the AAG-catalyzed single-turnover glycosylase reaction (k_{st}) was determined for 25 bp oligonucleotide duplexes containing a central Hx·T or ϵA·T mismatch at pH values ranging from 4.5 to 10 (Figure 2A,B). The pH−rate profiles for excision of both Hx and ϵA follow a bell-shaped curve with maximal activity around pH 6−6.5. Maximal activity occurs at pH values well below those previously used to assay AAG glycosylase activity (pH 7.5−8) so that the true catalytic prowess of this enzyme had been underestimated. The limiting slopes of 1 and −1 for the acidic and basic limbs, respectively, of the pH−rate profile indicate that the active form of the AAG·DNA complex is controlled by two essential ionizations. One group must be deprotonated for maximal activity (e.g., a general base), and the other must be protonated (e.g., a general acid). This model is presented in Scheme 2, and it is described by eq 2 (Experimental Procedures). The apparent pK_a values for the active AAG·DNA complex were obtained from nonlinear least-squares fits of eq 2 to the data in panels A and B of Figure 2 (Table 1). In the absence of additional information about the true ionization constants for the catalytic groups, it is possible that the pK_a of the acid group corresponds to either the higher pK_a value (p$K_{a2'}$, normal protonation) or the lower pK_a value (p$K_{a1'}$, reverse protonation; see ref *21* for an explanation of reverse protonation).[2]

The log-linear increase in activity on the alkaline limb of the pH−rate profile for excision of ϵA and Hx is reminiscent of acid-catalyzed nonenzymatic depurination, suggesting that AAG employs general acid catalysis to stabilize the purine leaving group. We tested this hypothesis by measuring the pH−rate profile for AAG-catalyzed excision of 7MeG.

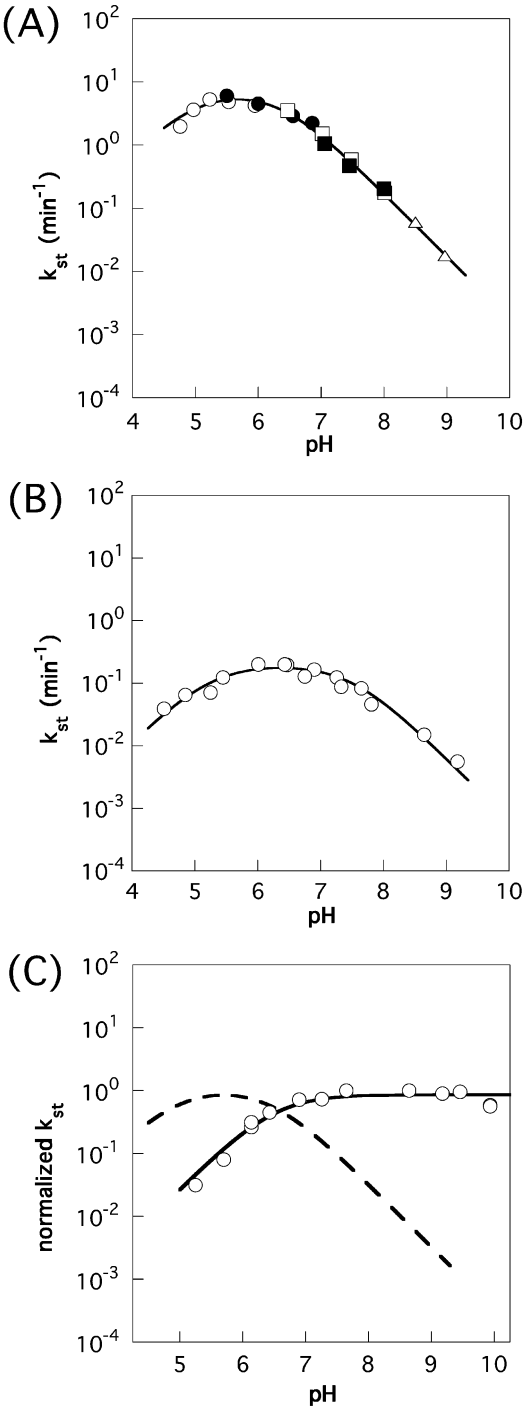

FIGURE 2: pH dependence of the single-turnover reaction catalyzed by AAG showing the involvement of acid−base catalysis. (A) For excision of hypoxanthine (Hx•T), pK_a values of 5.0 ± 0.2 and 6.4 ± 0.2 were obtained by nonlinear least-squares fitting of the model for two essential ionizations (Scheme 2 and eq 2). Different buffers were used at overlapping pH ranges [(○) sodium acetate, (●) NaMES, (□) NaMOPS, (■) NaHEPES, and (△) NaCHES]. (B) For excision of ϵA (ϵA•T), pK_a values of 5.3 ± 0.2 and 7.5 ± 0.2 were obtained (eq 2). (C) For excision of 7MeG (7MeG•C), a single pK_a value of 6.5 ± 0.1 was observed (eq 1). To facilitate comparison, the data for 7MeG (○) and Hx (− − −) are shown after normalization to the maximal rate for each substrate.

Methylation of N7 places positive charge on the purine ring at neutral pH, thereby rendering it a much better leaving group than a neutral purine nucleotide. The spontaneous depurination of 7-methylguanosine is ~10^4-fold faster than depurination of unmethylated guanosine at pH 7, and the hydrolysis of 7-methylguanosine is pH-independent across a wide range (*22*). If the essential proton in the AAG-catalyzed reaction functions to stabilize the leaving group, then the rate of 7MeG excision should be pH-independent in the alkaline region, as this substrate is already activated for reaction. Consistent with these expectations, the pH−rate profile for the single-turnover excision of 7MeG shows only a single rate-controlling deprotonation and a maximal reaction rate that is independent of pH from pH 7 to 10 (Figure 2C). This pH-independent plateau could result from a large shift in the pK_a of this catalytic group when a cationic substrate (7MeG) is bound, relative to its pK_a when a neutral substrate (Hx) is bound. However, simple electrostatic considerations would predict a decrease, rather than an increase, in the pK_a of an essential protonated group (i.e., the proximity of the positively charged group would make it more difficult to protonate this group). Therefore, we instead favor the interpretation that an acidic group that is required for the excision of neutral substrates is no longer required for the excision of a positively charged, activated substrate.

The observed pK_a value for excision of 7MeG (6.5 ± 0.1) is the same as the value of p$K_{a2'}$ (6.4 ± 0.2) for excision of Hx and substantially above the value of the first pK_a for the excision of Hx (p$K_{a1'}$ = 5.0 ± 0.2; Figure 2C and Table 1). This observation is most simply interpreted by the assignment of p$K_{a1'}$ to the ionization of a general acid that is required only for the reaction of neutral purine substrates and the assignment of p$K_{a2'}$ to the ionization of a general base that is required for the reaction of both charged and uncharged substrates [i.e., a reverse protonation model (*21*)].[2] The crystal structure of AAG suggests that Glu125 is the best candidate for the catalytic base (*3*, *4*), and functional evidence supporting this assignment is presented below.

Table 1: Summary of pK_a Values for AAG-Catalyzed Excision of Different Lesions[a]

excised base	pH dependence of k_{cat}/K_m			pH dependence of k_{st}	
	pK_{a1}	pK_{a2}	pK_{a3}	p$K_{a1'}$	p$K_{a2'}$
ϵA	ND[b]	ND[b]	ND[b]	5.3 ± 0.2	7.3 ± 0.2
7MeG	≤5[c]	6.0 ± 0.2[c]	7.9 ± 0.2	≤5[c]	6.5 ± 0.1[c]
Hx	5.4 ± 0.2	(6.0)[d]	(7.9)[d]	5.0 ± 0.2	6.4 ± 0.2

[a] The individual ionizations are shown in Scheme 2, and the pK_a values were determined from nonlinear least-squares fits of the model to the data in Figures 1 and 2. [b] Not determined. [c] From pH 5 to 10, only a single ionization was observed for k_{st} and only two ionizations were observed for k_{cat}/K_m. pK_a values (Scheme 2) are assigned according to the reverse protonation model (see footnote 2 in the text). [d] To obtain the value of pK_{a1} from eq 4, the values of pK_{a2} and pK_{a3} were assigned from the pH dependence for excision of 7MeG (Figure 2A).

[2] We have tentatively assigned the kinetic pK_a values according to a reverse protonation model, because the pK_a value observed for excision of 7MeG is more similar to p$K_{a2'}$ than to p$K_{a1'}$ (Table 1). A normal protonation model cannot be excluded, provided the pK_a values of the catalytic groups were different in the presence of different bound substrates. For example, p$K_{a2'}$ is ~1 pH unit higher for the excision of ϵA than for the excision of Hx. The pH dependencies for k_{cat}/K_m (free enzyme) are also adequately fit by the reverse protonation model, although the pK_a values for Hx are too similar to be fit independently (Figure 3B and Table 1). This assignment of reverse protonation does not affect our conclusions; a definitive assignment will require identification of the ionizing catalytic groups and direct measurement of their pK_a values.

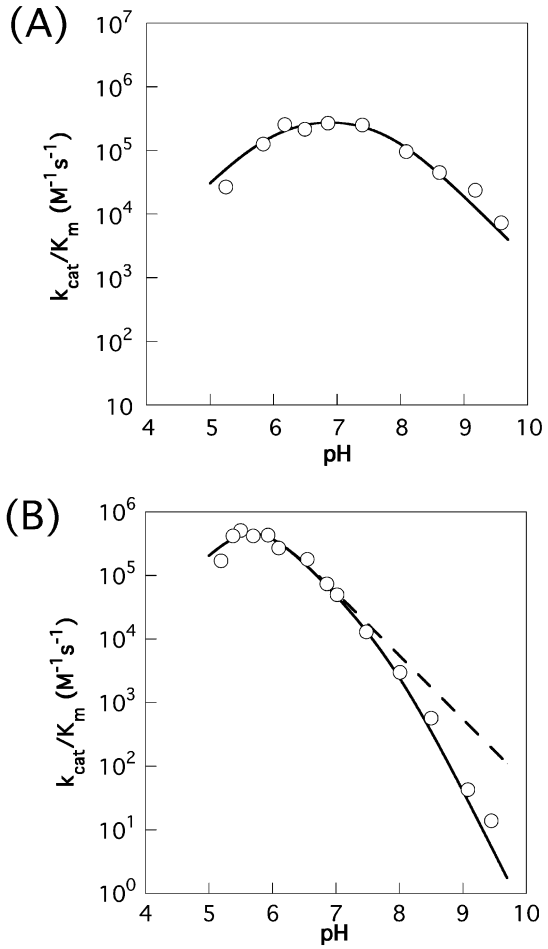

FIGURE 3: pH dependence of k_{cat}/K_m for the AAG-catalyzed reaction revealing an additional titratable group. (A) For release of 7MeG from a DNA substrate (7MeG·C), pK_a values of 6.0 ± 0.2 and 7.9 ± 0.2 were obtained (eq 3). (B) For Hx release, the data are not well fit by eq 3 (− − −) and show a marked deviation at higher pH values. The data are better fit by inclusion of an additional ionization with a pK_{a1} value of 5.4 ± 0.2 [eq 4 (—)], after fixing the values of pK_{a2} (6.0) and pK_{a3} (7.9) to the values determined for the 7MeG substrate in panel A. The presence of two essential protonated groups results in a slope of −2 for the basic limb of the pH−rate profile.

pH Dependence for k_{cat}/K_m. The pH dependencies for the single-turnover reactions reflect ionizations of enzyme·substrate complexes, making it difficult to compare the pK_a values observed with different substrates. Therefore, the pH dependence of k_{cat}/K_m was also determined for excision of Hx and 7MeG to address whether the same catalytic groups are required for reaction with positively charged (i.e., activated) and neutral (i.e., stable) substrates and to identify any additional ionizable groups that might be involved in DNA binding. The dependence of k_{cat}/K_m on pH reflects the ionizations of the unbound substrate and enzyme. Since the DNA substrate lacks ionizable groups with pK_a values in the pH range of 5−9, there is a strong expectation that any ionizations observed under k_{cat}/K_m conditions reflect titratable protein groups.

The pH dependence for k_{cat}/K_m with 7-methylguanosine-containing DNA is shown in Figure 3A. In contrast to the single pK_a observed for the single-turnover reaction [Figure 2C (○)], the pH−rate profile for k_{cat}/K_m follows a bell-shaped curve with a slope of 1 on the acidic limb and a slope of −1 on the alkaline limb (Figure 3A). The decrease in k_{cat}/K_m at higher pH reveals the presence of an enzymatic group that must be protonated for substrate binding or, in principle, for catalysis. However, the appearance of this ionization only under subsaturating conditions strongly suggests that it reflects a group involved in DNA binding rather than catalysis. We have assigned this ionization to K_{a3} (Scheme 2). If this interpretation is correct, then other substrates should require protonation of the same enzymatic group for DNA binding to occur, in addition to any protonation required for the activation of substrates with neutral leaving groups. For neutral substrates, the alkaline limb of the pH dependence should exhibit a slope of −2 under subsaturating conditions.

The pH dependence of k_{cat}/K_m for AAG-catalyzed excision of Hx is shown in Figure 3B. The equation for two essential ionizations that describes the pH dependence of 7MeG excision (eq 3 and Figure 3A) does not fit the data for Hx excision [Figure 3B (− − −)]. Instead, the alkaline limb of the pH−rate profile is better fit by a slope of −2 above pH 8. This indicates the involvement of two essential protonated groups in the reaction with Hx [Figure 3B (—) and eq 4]. Using the previously determined values of pK_{a2} (6.0) and pK_{a3} (7.9) for the reaction of 7MeG, the pH dependence of the Hx reaction is readily fit after including a third protonation (pK_{a1} = 5.4). This pK_a value for the essential acidic group in the free enzyme is similar to the pK_a values of 5.3 and 5.0 that were observed for reaction of the E·S complex with ϵA and Hx, respectively (Table 1). This observation would suggest that the pK_a of the proposed general acid is not markedly perturbed by substrate binding. The dependence of k_{cat}/K_m for excision of both 7MeG and Hx on an additional proton that was not observed for single-turnover (k_{st}) conditions is consistent with a protonated group that is important for DNA binding.

The requirement for an additional protonated group in the reaction of ϵA and Hx, but not in the reaction of 7MeG, is compelling evidence for general acid catalysis in the excision of neutral nucleobases. This difference reveals itself in the bell-shaped pH−rate profile for k_{st} with neutral substrates versus the single inflection for 7MeG (Figure 2) and in the slope of −2 for the alkaline limb of the pH−rate profile for k_{cat}/K_m with Hx versus the slope of −1 for the alkaline limb with 7MeG (Figure 3).

Requirement of the Purine N7 for AAG-Catalyzed Excision. To test whether leaving group protonation is required for activation of damaged purines with stable *N*-glycosidic bonds, we prepared an oligonucleotide containing a modified deoxyinosine substrate with carbon substituted for the 7-nitrogen of the purine ring (7-deazainosine; 7-deazahypoxanthine nucleobase, Scheme 1). The base pairing properties of 7-deazainosine are very similar to those of inosine, but it lacks the 7-nitrogen group and hence cannot be readily protonated (*23*). If AAG activity depends on protonation of the 7-nitrogen for stabilization of neutral leaving groups, then 7-deazainosine should be a poor substrate. No glycosylase activity was detected toward 7-deazainosine·T even after long incubation times ($k_{st} \leq 3 \times 10^{-6}$ min^{-1}; data not shown), corresponding to a decrease in activity of more than 10^7-fold relative to that for the reaction of inosine. The 7-deaza analogue of inosine is extremely resistant to acid-catalyzed depurination, presumably because protonation normally occurs at N7 of inosine (*24*). The similarly large deleterious

effect of N7 substitution on AAG-catalyzed *N*-glycosidic bond hydrolysis is consistent with a similar acid-catalyzed mechanism for the enzymatic glycosylase reaction (*25*, *26*).[3] N7 of the substrate is a good candidate for the site of protonation, but these data do not provide a definitive assignment. Protonation at either N7 or N3 of the nucleobase would constitute a reasonable pathway for general acid catalysis, although protonation of the bridging N9 is less likely for steric reasons.

AAG Binds to Pyrimidine Mismatches, but Cannot Catalyze Their Excision. Prokaryotic and eukaryotic cells both possess 3-methyladenine DNA glycosylases with broad substrate specificities that excise damaged bases differing in size, charge, and hydrogen bonding ability (Scheme 1). For example, *E. coli* AlkA recognizes various alkylation and oxidation adducts of both purine and pyrimidine bases (*27*). Both AAG and AlkA are capable of removing normal purines from DNA, albeit very slowly with some preference for substrates in mismatched base pairs (*1*, *28*, *29*). AlkA also removes normal pyrimidines, whereas no such activity has been detected for AAG (*5*, *28*). However, previous studies of AAG and related mammalian enzymes measured activity at alkaline pH, and it is possible that pyrimidine excision might be detectable at the pH optimum of approximately 6. To evaluate whether the strict preference for purines is a unique feature of the mammalian enzyme, we tested whether AAG can catalyze the excision of normal pyrimidines from DNA.

AAG binds to DNA oligonucleotides containing a mismatched pyrimidine·pyrimidine base pair with K_d values of 2−20 nM (data not shown), consistent with a previous report (*5*). Given this tight binding, which is similar to the binding of ϵA [K_d values of 0.2−20 nM (*5*, *17*)], it is likely that a flipped-out pyrimidine is stabilized by AAG in these complexes. Nevertheless, no glycosylase activity was detected toward cytidine, thymidine, or uridine, even after incubation for several days at pH values ranging from 5 to 8 ($k_{st} \leq 3 \times 10^{-6}$ min^{-1}). Under these same conditions, AAG catalyzes the excision of the normal purines guanine and adenine from mismatches with rate constants of 10^{-3}−10^{-5} min^{-1} (data not shown). Although AAG recognizes the distortion in the DNA duplex caused by a pyrimidine·pyrimidine mismatch and can presumably bind pyrimidine nucleosides in the active site, pyrimidines are not substrates for base excision. This selection at the bond cleavage step for purines and against pyrimidines is in marked contrast to the ability of *E. coli* AlkA to remove both purines and pyrimidines (*27*, *28*, *30*). This difference in substrate range suggests some fundamental differences in the catalytic mechanisms of the 3-methyladenine DNA glycosylases AAG and AlkA.

What Is the Identity of the General Acid? The different pH dependencies for the excision of positively charged and neutral purines (Figure 2C) strongly suggest that neutral leaving groups are stabilized by protonation or by hydrogen bond donation. Crystal structures of AAG bound to DNA identify only a handful of protein side chains in the vicinity of the bound nucleobase that are capable of functioning as a general acid (Figure 4 and refs *3* and *4*). Although no hydrogen bonds are observed between the ring nitrogen atoms of the bound ϵA and the candidate acidic residues, a movement of a few angstroms could bring several different side chains into position for proton transfer or proton transfer could be mediated by an intervening water molecule. We considered each of these candidate residues and investigated them by mutation. The results suggest that none of these residues functions as the general acid, leaving unanswered the question of which group protonates the leaving group during AAG-catalyzed base excision.

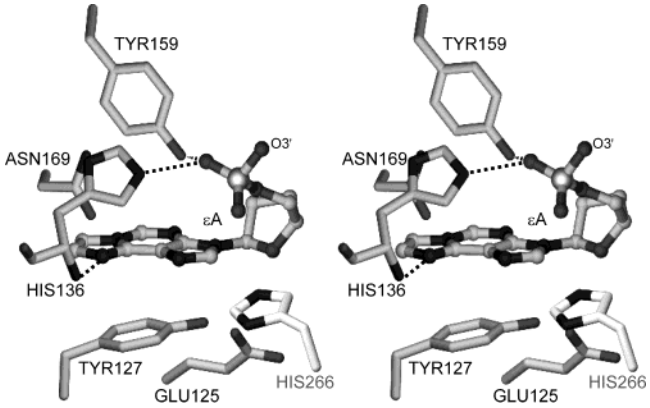

FIGURE 4: Stereoview of the base binding pocket of AAG from the crystal structure of AAG bound to an ϵA-containing DNA (*4*), showing the residues that were mutated (Table 2). The position of His266, taken from the structure of AAG bound to a pyrrolidine−DNA inhibitor (*3*), was obtained by superposition of all protein atoms of the pyrrolidine and ϵA complexes.

Perhaps the best candidate for the general acid that is observed in the crystal structure is the imidazolium group of His136, which is within 3.8 Å of N7 of the bound ϵA (Figure 4). The possibility of His136 serving as the general acid was tested by mutating this amino acid to glycine, alanine, and glutamine. The predicted phenotype of a general acid mutant would be greatly decreased glycosylase activity toward neutral purine lesions accompanied by a shift in the pH−rate profile (the ionization corresponding to the general acid might be expected to shift to the pK_a of the substrate DNA itself, which is expected to be in the range of 2−4). Since protonation is not necessary for excision of 7MeG, mutation of the general acid should have little or no effect on activity toward this substrate. Given that His136 contacts the DNA backbone immediately 5′ of ethenoadenosine in the crystal structure, it was expected that mutations at this position could have a deleterious effect on DNA binding even if His136 does not act as a general acid. The activities of the His136 mutants in single-turnover excision show only a modest decrease in the rate of ϵA excision (8−40-fold) and a larger decrease in the rate of 7MeG excision (30−4000-fold). The pH−rate profile for single-turnover excision of ϵA shifts by ∼1 pH unit relative to that of the wild type, but the same shift was observed for excision of 7MeG (Figure 5). The greater loss of activity toward 7MeG than toward ϵA is the opposite of the behavior expected if H136 were serving as a general acid in the excision of ϵA. These data suggest that His136 plays another role, such as positioning

[3] While consistent with the protonation model, the inability of AAG to excise 7-deazahypoxanthine does not constitute proof of protonation at the N7 position. It is possible that substitution at N7 has another deleterious effect, such as removing a hydrogen bond acceptor that helps to position the substrate, or that the reduced ability of 7-deazahypoxanthine to stabilize developing negative charge is responsible for its resistance to hydrolysis.

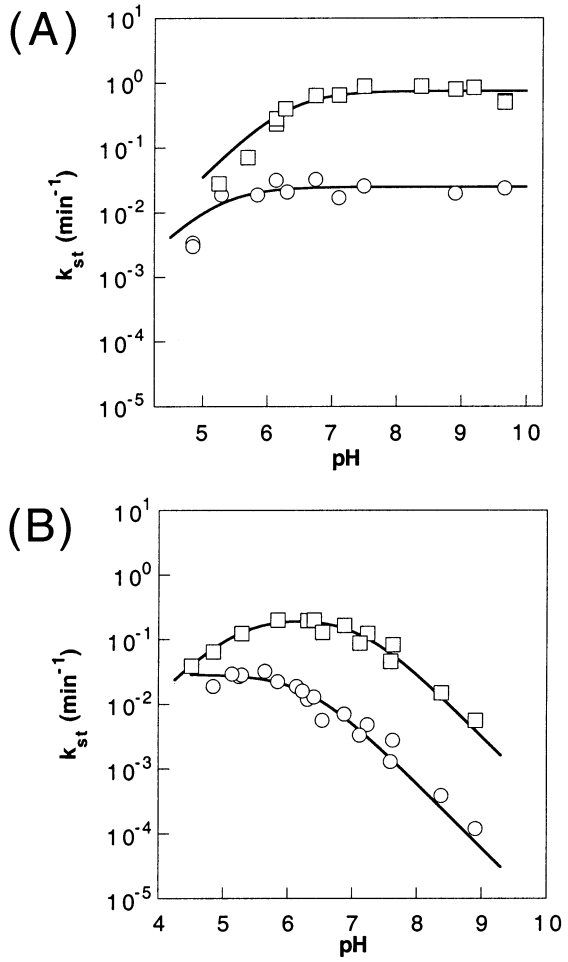

FIGURE 5: pH dependence for single-turnover excision of ϵA and 7MeG by H136Q AAG. The single-turnover glycosylase activity of H136Q AAG (○) was measured as a function of pH and compared to the data for wild-type AAG (□) from Figure 1. (A) For the excision of ϵA (ϵA·T) by H136Q AAG, only a single pK_a value of 6.6 ± 0.2 could be observed because of the instability of the mutant enzyme at low pH (eq 2; p$K_{a2'}$ was not observed). (B) For excision of 7MeG (7MeG·C), a pK_a value of 5.3 ± 0.3 was obtained (eq 1). The small decrease in k_{st} and modest shift in the pK_a value for the mutant enzyme acting on either substrate suggest that His136 does not function as the critical general acid.

the substrate for reaction. The smaller deleterious effect of the His136 mutations on excision of ϵA than on the excision of 7MeG could indicate that the bound ϵA substrate is stabilized by additional binding interactions with the bulky etheno adduct that are not available to the smaller 7MeG substrate.

Tyr127 and Tyr159 in the active site of AAG have their hydroxyl groups positioned within 4 Å of ring nitrogen atoms of ϵA (Figure 4). Neither the alignment nor the distance of these side chains is appropriate for proton transfer to ϵA, but a small adjustment of these side chains could align either residue to serve as a general acid. These tyrosines were individually mutated to tryptophan to remove the potential proton donor while preserving any aromatic stacking interactions with the substrate. The mutants Y127W and Y159W retain near-wild-type activities, with only 3- and 10-fold reductions, respectively, in the single-turnover rates of ϵA excision (Table 2). These results suggest that neither Tyr127 nor Tyr159 is the general acid that was revealed by the pH dependencies of the glycosylase reaction.

Table 2: Single-Turnover *N*-Glycosylase Activity of Wild-Type and Mutant Δ80 AAG[a]

enzyme	1,N^6-ethenoadenine k_{st} (min^{-1})[b]	fold decrease	7-methylguanine k_{st} (min^{-1})[c]	fold decrease
wild-type	1.6×10^{-1}	(1)	0.8	~(1)
H266A	1.0×10^{-1}	1.6	1.3	0.62
Y159W	6.0×10^{-2}	2.7	1.0×10^{-3}	800
Y127W	2.0×10^{-2}	8	4.5×10^{-2}	18
H136Q	2.0×10^{-2}	8	3.0×10^{-2}	27
H136A	1.0×10^{-2}	16	5.0×10^{-3}	160
H136G	4.0×10^{-3}	40	2.0×10^{-4}	4000
E125Q	$\leq 1 \times 10^{-5}$	≥16000	$\leq 1 \times 10^{-4}$	≥8000
E125A	$\leq 1 \times 10^{-5}$	≥16000	$\leq 1 \times 10^{-4}$	≥8000
E125D	1.3×10^{-2}	12	3.0×10^{-2}	27
E125C	4.0×10^{-5}	4000	2.0×10^{-4}	4000

[a] Rate constants for the single-turnover reaction with 25mer oligonucleotide duplexes containing a central ϵA·T or 7MeG·C base pair were determined at 37 °C with 50 mM buffer, 10% glycerol, 0.1 mg/mL BSA, 1 mM DTT, and 1 mM EDTA and a constant ionic strength of 0.1 M, maintained with NaCl. In all cases, the protein was in excess over DNA, with at least 10-fold more protein than DNA, and the concentration of protein was varied over a 10−1000-fold range to ensure that the DNA substrate was saturated. Each value reflects the average of at least three independent experiments, and the standard deviation was less than 20% of the value of the mean. The deleterious effect of the mutation is given by the fold decrease, calculated as the ratio of the rate constant for the wild type divided by the rate constant for the mutant. [b] In NaMES at pH 6.0. [c] In NaCHES at pH 9.0.

An additional candidate for the general acid, His266, contacts the backbone phosphoryl group of the flipped-out nucleotide in the structure of AAG bound to a pyrrolidine abasic DNA inhibitor (*3*). Although no base is present in this structure, the histidine side chain (Figure 4) is within 6 Å of the base-binding pocket that was identified in another crystal structure with a bound ϵA substrate (*4*). In the AAG·ϵA DNA complex, the loop containing His266 has moved away from the active site, calling into question whether this residue plays a role in DNA binding or catalysis. We mutated His266 to alanine and serine to test the possibility that His266 participates in the chemical step as the general acid. Both of these mutants retained nearly wild-type levels of single-turnover glycosylase activity, ruling out the possibility that His266 is the general acid (Table 2).

Our failure to identify the general acid by mutagenesis on the basis of the crystal structure raised the possibility that there are multiple pathways for protonation of the nucleobase in the AAG active site. If this were true, then mutation of the primary general acid might not produce an obvious phenotype. Multiple pathways for proton transfer have been proposed for water-mediated proton transfer in the reactions of carbonic anhydrase (*31*) and a transformylase (*32*). Alternatively, the complexes observed in the crystal structures of AAG may require a structural rearrangement to obtain the reactive complex. Such a rearrangement might bring a more distant general acid residue into the active site. The observation that the ϵA-containing DNA substrate is not cleaved in the crystal structure of the wild-type enzyme could indicate that such a rearrangement is required (*4*).

Evidence for Glu125 Serving as the General Base. It was previously proposed that Glu125 positions and activates a nucleophilic water molecule and mutation of this residue to Gln or Ala resulted in undetectable *N*-glycosylase activity both *in vivo* and *in vitro* (*4*). This makes Glu125 a good candidate for the deprotonated catalytic group that controls

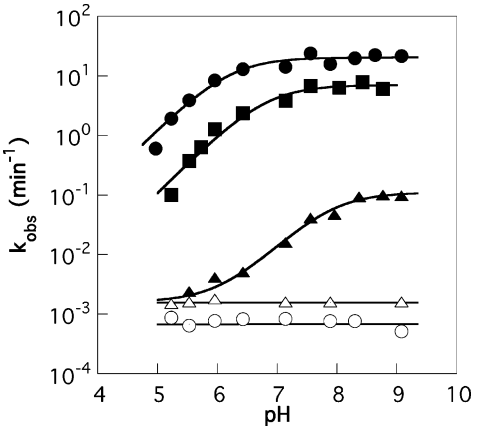

FIGURE 6: Evidence that Glu125 is the catalytic base in the AAG-catalyzed reaction. The pH dependencies for single-turnover excision of 7MeG (7MeG·T) by wild-type (●), E125D (■), E125C (▲), and E125A AAG (△) are shown. The greater activity of AAG toward a mismatched 7MeG·T substrate facilitated detection of the low level of activity of the E125C mutant. The rate of spontaneous hydrolysis for the 7MeG·T mismatch was also measured and is shown for comparison (○). The E125A mutant exhibited only slight elevation of glycosylase activity over the uncatalyzed reaction. The apparent pK_a values for wild-type and E125D AAG are 6.0 ± 0.2 and 6.4 ± 0.2, respectively (eq 1). As the pH dependence for the E125C mutant appeared to plateau at low pH values, these data were fit to eq 5 (see Experimental Procedures) with a pK_a value of 7.9 ± 0.2.

the activity of AAG. We constructed several mutations at position 125 and examined the pH−rate profiles of the mutants to test this proposal. Gel shift experiments confirmed that both the E125Q and E125A mutants bind efficiently to DNA lesions (ref *17* and data not shown), and the crystal structure of the E125Q mutant bound to ϵA-containing DNA is essentially identical to the structure of wild-type AAG bound to the same DNA (*4*). However, no glycosylase activity could be detected at pH values ranging from 5 to 9 for either mutant even after long incubation times (up to several days), indicating that the activities of the mutants are at least 10^4-fold lower than the activity of wild-type AAG (Table 2). The large deleterious effect of mutating Glu125 indicates that it is indeed a critical residue for catalysis (*4*).

The more conservative mutation of Glu125 to either Asp or Cys resulted in mutant proteins with reduced levels of glycosylase activity (Table 2). Aspartate (E125D) was the best replacement for glutamate, with only 10−30-fold reductions in single-turnover glycosylase activity for excision of ϵA and 7MeG. The E125C mutant was more severely compromised, but it did exhibit detectable levels of glycosylase activity (~10^3-fold less than wild-type AAG). To measure the pH dependence of 7MeG excision for the E125 mutants, we utilized a 7MeG·T mismatch because AAG has a 20-fold greater turnover rate for a 7MeG·T mismatch than for a 7MeG·C base pair. The higher level of activity toward the mismatched 7MeG·T substrate allowed the low level of activity of the E125C mutant to be more readily detected. The pH dependence for 7MeG excision is similar for the E125D and wild-type enzymes, suggesting that the mutant has an analogous catalytic mechanism (Figure 6). The reduced rate constant of E125D can be explained by suboptimal placement of the catalytic carboxylate. The E125C mutant exhibits a significantly higher pK_a value (7.9 ± 0.2) that is consistent with the expected pK_a of a thiolate.

Scheme 3

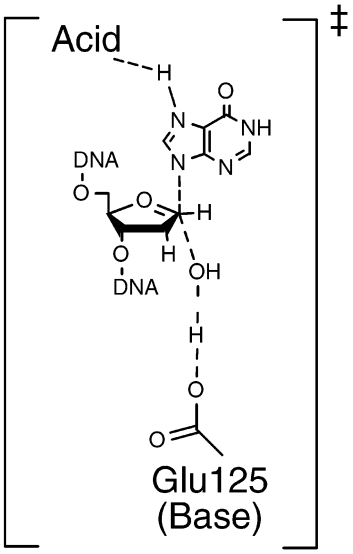

The shift in the pH−rate profile of the E125C mutant strongly suggests that Glu125 is deprotonated in the active form of the enzyme, and it is the protonation of this carboxylate that leads to the loss of activity at acidic pH. These observations are consistent with the proposal that Glu125 acts as a general base to activate and position a nucleophilic water molecule (*4*).

An Acid−Base-Catalyzed Mechanism for AAG-Catalyzed N-Glycosidic Bond Hydrolysis. The pH dependence for the AAG-catalyzed reaction reveals the presence of two essential catalytic groups, one of which must be deprotonated and one which must be protonated for maximal activity (Scheme 3). Mutagenesis and the altered pK_a of the E125C mutant implicate Glu125 as the essential deprotonated catalytic group, and the structural analysis favors a role in positioning and activating the nucleophilic water. A general acid, as yet unidentified, acts to protonate the nucleobase leaving group. Below, we consider the contributions from acid−base catalysis in the context of the overall ~10^8-fold rate enhancement for AAG-catalyzed hydrolysis of deoxyinosine-containing DNA (see Experimental Procedures).

The catalytic contribution from the general base can be approximated as ~10^4-fold, based upon the decreased activity of the E125Q and E125A mutant proteins. This contribution is larger than expected for chemical activation of a nucleophile participating in a dissociative oxocarbenium ion-like transition state. However, this value is similar to the 10^2−10^3-fold deleterious effect of substituting the residue proposed to act as the general base in uracil DNA glycosylase (D64N), an enzyme that stabilizes a highly dissociative transition state (*11, 13*). In addition to activating the water nucleophile, which is expected to have a modest effect on a dissociative transition state, Glu125 may play a more important role in positioning it for attack at the anomeric carbon of the substrate. Similar large rate accelerations have been attributed to positioning of a nucleophile within an active site. For example, a 100-fold catalytic advantage has been attributed to positioning of the nucleophile by NDP kinase, an enzyme that catalyzes phosphoryl transfer via a dissociative transition state (*33*).

The catalytic contribution of AAG's general acid can be estimated to be ~10^4-fold from the observed decrease in the

reaction rate as a function of pH. The single-turnover rate constant decreases by $\sim 10^3$-fold between pH 6 and 9, and an additional factor of 10 can be attributed to reverse protonation (i.e., $pK_{a1'}$ and $pK_{a2'}$ are $\sim$1 pH unit apart, and with reverse protonation only 10% of the enzyme is in the active form at the pH optimum). Together, general acid and general base catalysis can account for much of the $\sim 10^8$-fold rate advantage realized by AAG. It is unlikely that these are the only contributions to catalysis, and the two $\sim 10^4$-fold effects that we have ascribed to general acid and general base catalysis are unlikely to be strictly additive. Nonadditivity, which can be attributed to a cooperative network of catalytic interactions, is commonplace in enzyme active sites (e.g., refs *34* and *35*). It is remarkable that no candidates for electrostatic stabilization of an oxocarbenium ion-like transition state have been identified for AAG, as C1′ and O4′ are expected to undergo the most extensive change in effective charge in going from the ground state to the transition state. Two positively charged abasic DNA analogues, pyrrolidine (4-azaribose) and 1-azaribose, mimic the expected positive charge that would develop in an oxocarbenium ion-like transition state, and both of these are tight binding inhibitors of AAG (ref *36* and unpublished results). However, the crystal structure of AAG bound to the pyrrolidine-containing DNA did not reveal any specific contacts between the 4-aza group and the protein that would be consistent with electrostatic stabilization of the positively charged sugar (*3*). This observation raises the possibility that the tighter binding of a positively charged abasic analogue might be achieved via longer-range electrostatic interactions, perhaps with the negatively charged phosphoryl groups of the DNA. Such an electrostatic interaction would be expected to stabilize the transition state for *N*-glycosidic bond hydrolysis. It has been proposed that uracil DNA glycosylase might use an electrostatic contribution from the DNA phosphoryl groups to stabilize the developing positive charge on the sugar in the transition state (*37*, *38*).

General acid catalysis can explain the discrimination of AAG against pyrimidine nucleosides, while permitting the reaction of structurally diverse purine nucleosides. Given that general acid catalysis is capable of accelerating the reaction of modified and unmodified purines to similar extents, it seems likely that AAG discriminates against normal purines on the basis of their shape and hydrogen bonding ability (*4*, *17*). A similar strategy of general acid catalysis has been reported for an RNA glycosylase and for nucleoside hydrolases that act on free nucleosides (*39*, *40*). The widespread use of general acid catalysis by evolutionarily diverse enzymes attests to the fitness of this mechanism, and it suggests that other DNA repair glycosylases acting on purine substrates (*25*) might also employ general acid catalysis.

ACKNOWLEDGMENT

We thank T. Biswas and J. Chang for expression plasmids, B. Eichman for assistance with Figure 4, and S. Admiraal and D. Herschlag for critical comments on the manuscript.

SUPPORTING INFORMATION AVAILABLE

Single-turnover glycosylase activity for full-length, Δ80, and Δ79 AAG proteins. This material is available free of charge via the Internet at http://pubs.acs.org.

REFERENCES

1. Wyatt, M. D., Allan, J. M., Lau, A. Y., Ellenberger, T. E., and Samson, L. D. (1999) *BioEssays 21*, 668−676.
2. McCullough, A. K., Dodson, M. L., and Lloyd, R. S. (1999) *Annu. Rev. Biochem. 68*, 255−285.
3. Lau, A. Y., Scharer, O. D., Samson, L., Verdine, G. L., and Ellenberger, T. (1998) *Cell 95*, 249−258.
4. Lau, A. Y., Wyatt, M. D., Glassner, B. J., Samson, L. D., and Ellenberger, T. (2000) *Proc. Natl. Acad. Sci. U.S.A. 97*, 13573−13578.
5. Biswas, T., Clos, L. J., II, SantaLucia, J., Jr., Mitra, S., and Roy, R. (2002) *J. Mol. Biol. 320*, 503−513.
6. Panzica, R. P., Rousseau, R. J., Robins, R. K., and Townsend, L. B. (1972) *J. Am. Chem. Soc. 94*, 4708−4714.
7. Bzowska, A., Kelikowska, E., and Shugar, D. (1993) *Z. Naturforsch. 48*, 803−811.
8. Garrett, E. R., and Mehta, P. J. (1972) *J. Am. Chem. Soc. 94*, 8532−8541.
9. Zoltewicz, J. A., Clark, D. F., Sharpless, T. W., and Grahe, G. (1970) *J. Am. Chem. Soc. 92*, 1741−1750.
10. Oivanen, M., Hovinen, J., Lehikoinen, P., and Lonnberg, H. (1993) *Trends Org. Chem. 4*, 397−412.
11. Drohat, A. C., Jagadeesh, J., Ferguson, E., and Stivers, J. T. (1999) *Biochemistry 38*, 11866−11875.
12. Stivers, J. T., Pankiewicz, K. W., and Watanabe, K. A. (1999) *Biochemistry 38*, 952−963.
13. Werner, R. M., and Stivers, J. T. (2000) *Biochemistry 39*, 14054−14064.
14. Shapiro, R., and Danzig, M. (1972) *Biochemistry 11*, 23−29.
15. Miroux, B., and Walker, J. E. (1996) *J. Mol. Biol. 260*, 289−298.
16. Asaeda, A., Ide, H., Asagoshi, K., Matsuyama, S., Tano, K., Murakami, A., Takamori, Y., and Kubo, K. (2000) *Biochemistry 39*, 1959−1965.
17. Abner, C., Lau, A. Y., Ellenberger, T., and Bloom, L. B. (2001) *J. Biol. Chem. 276*, 13379−13387.
18. O'Connor, T. R. (1993) *Nucleic Acids Res. 21*, 5561−5569.
19. Petronzelli, F., Riccio, A., Markham, G. D., Seeholzer, S. H., Stoerker, J., Genuardi, M., Yeung, A. T., Matsumoto, Y., and Bellacosa, A. (2000) *J. Biol. Chem. 275*, 32422−32429.
20. Porello, S. L., Leyes, A. E., and David, S. S. (1998) *Biochemistry 37*, 14756−14764.
21. Joshi, M. D., Sidhu, G., Pot, I., Brayer, G. D., Withers, S. G., and McIntosh, L. P. (2000) *J. Mol. Biol. 299*, 255−279.
22. Hendler, S., Furer, E., and Srinivasan, P. R. (1970) *Biochemistry 9*, 4141.
23. Seela, F., and Mittelbach, C. (1999) *Nucleosides Nucleotides 18*, 425−441.
24. Saladino, R., Mincione, E., Crestini, C., Negri, R., Mauro, E. D., and Costanzo, G. (1996) *J. Am. Chem. Soc. 118*, 5615−5619.
25. Porello, S. L., Williams, S. D., Kuhn, H., Michaels, M. L., and David, S. S. (1996) *J. Am. Chem. Soc. 118*, 10684−10692.
26. Jiricny, J., Ubasawa, A., and Wood, S. (1985) *Nucleosides Nucleotides 4*, 205−207.
27. McCarthy, T. V., Karran, P., and Lindahl, T. (1984) *EMBO J. 3*, 545−550.
28. Berdal, K. G., Johansen, R. F., and Seeberg, E. (1998) *EMBO J. 17*, 363−367.
29. Connor, E. E., and Wyatt, M. D. (2002) *Chem. Biol. 9*, 1033−1041.
30. Saparbaev, M., and Laval, J. (1994) *Proc. Natl. Acad. Sci. U.S.A. 91*, 5873−5877.
31. Tu, C., Qian, M., An, H., Wadhwa, N. R., Duda, D., Yoshioka, C., Pathak, Y., McKenna, R., Laipis, P. J., and Silverman, D. N. (2002) *J. Biol. Chem. 277*, 38870−38876.
32. Warren, M. S., Marolewski, A. E., and Benkovic, S. J. (1996) *Biochemistry 35*, 8855−8862.
33. Admiraal, S. J., Schneider, B., Meyer, P., Janin, J., Veron, M., Deville-Bonne, D., and Herschlag, D. (1999) *Biochemistry 38*, 4701−4711.
34. Carter, P., and Wells, J. (1988) *Nature 332*, 564−568.

35. Weber, D. J., Serpersu, E. H., Shortle, D., and Mildvan, A. S. (1990) *Biochemistry 29*, 8632−8642.
36. Scharer, O. D., Nash, H. M., Jirieny, J., Laval, J., and Verdine, G. L. (1998) *J. Biol. Chem. 273*, 8592−8597.
37. Dinner, A. R., Blackburn, G. M., and Karplus, M. (2001) *Nature 413*, 752−755.
38. Jiang, Y. L., Ichikawa, Y., Song, F., and Stivers, J. T. (2003) *Biochemistry 42*, 1922−1929.
39. Chen, X.-Y., Berti, P. J., and Schramm, V. L. (2000) *J. Am. Chem. Soc. 122*, 1609−1617.
40. Horenstein, B. A., Parkin, D. W., Estupinan, B., and Schramm, V. L. (1991) *Biochemistry 30*, 10788−10795.

BI035177V